J. Biochem. 2009;146(2)193–200
doi:10.1093/jb/mvp055

Effect of Metal Ion on the Structural Stability of Tumour Suppressor Protein p53 DNA-Binding Domain

Yonglai Xue, Shuai Wang and Xizeng Feng*
College of Life Science, Nankai University at Tianjin, P. R. China 300071

Received March 9, 2009; accepted March 24, 2009; published online April 3, 2009

The tumour suppressor protein p53 is a sequence-specific transcription factor that coordinates one molecule of zinc in the core domain. In our recent study, magnesium can also bind to the p53DBD and enhance its DNA-binding activity. In this study, a systematic analysis of the conformation and stability changes induced by these two metal ions was reported. The spectra of protein intrinsic fluorescence were used to measure the equilibrium unfolding of the p53DBD protein. The stability against chemical denaturation increased in the order apo < Mg^{2+} < Zn^{2+}. The thermal stability monitored by DSC scans showed that the binding of metal ions to p53DBD increased the thermal stability of the protein. To explore additional information of structural changes after the binding of metal ions, we used the fluorescent probes to evaluate the hydrophobic surface exposure. The results established that metal ions binding increased hydrophobic exposure on the surface of p53DBD. Analysis of acrylamide quenching experiments revealed that the binding of metal ions to p53DBD induced a structural modification of the protein and this change provided significant protection against acrylamide quenching. Overall, the present results indicated that p53DBD underwent a conformational change upon the binding of metal ions, which was characterized by an increased stability of the protein.

Key words: equilibrium unfolding, denature, fluorescence, conformational change, stability.

Abbreviations: ANS, 1-anilino-8-naphthalene sulphonate; DBD, DNA-binding domain; DSC, differential scanning calorimetry; DTT, dithiothreitol; GdmHCl, guanidinium hydrochloride; SDS, sodium dodecyl sulphate.

The tumour suppressor protein p53 is a sequence-specific transcription factor that functions to maintain the integrity of the genome (*1–3*). It acts as a potent transcription factor which is activated in response to a variety of DNA-damaging agents, and may lead to cell-cycle arrest at the G1/S phase checkpoint or induction of apoptosis (*4–10*). In addition, p53 also negatively regulates the transcription of genes containing TATA box-initiated promoters by binding to the protein components of the basal transcription machinery and thus is thought to be directly involved in checking DNA replication (*11–13*). Many studies have shown that all of these presently known biological functions of p53 depend critically upon its DNA-binding properties (*14–16*). Wild-type p53 binds DNA through a sequence-specific DNA-binding domain (p53DBD) extending from amino acid residues 96–308 (*17*). The high number of mutations is found in the sequence-specific DNA-binding domain and consequently cannot activate transcription (*4*, *18*). This fact strongly suggests that sequence-specific DNA binding and transactivation are the key activities that control the biological functions of p53 (*4*, *19*).

The crystal structure of p53DBD reveals that the p53 core domain structure consists of a beta sandwich that serves as a scaffold for two large loops (L2 and L3) and a loop–sheet–helix motif (L1) (Fig. 1) (*20–22*). Zn^{2+} is coordinated to C176 and H179 of the L2 loop and C238 and C242 of the L3 loop (*20*). The L1 loop forms the DNA-binding surface of p53. Zinc coordination is thought to be necessary for the proper folding of the p53 core domain *in vitro* and disruption of this interaction greatly reduces or abrogates p53 DNA binding and transactivation of target genes (*23–25*). NMR spectra reveal that the DNA-binding surface is altered by removing zinc ion and fluorescence anisotropy studies show that zinc ion removal abolishes site-specific DNA-binding activity, although full non-specific DNA-binding affinity is retained (*26*). Nevertheless, recombinant p53 polypeptide can specifically bind copper ions, results in disrupting the p53 conformation and its DNA-binding activity (*27–28*). These opposite effects of different metal ions on p53 support the notion that additional metal ions or cellular factors can affect the specific recognition. In our recent study (*29*), we found that magnesium ions could bind to the p53DBD protein and enhanced the DNA-binding affinity of p53DBD in a non-specific manner, which is different from that of zinc ions in a sequence-specific manner. We are thus interested in determining whether the binding of magnesium ions influence the structural stability of p53DBD.

In the present work, we examined the effect of these two metal ions on the structural stability of the p53DBD. We demonstrate that the stability of p53DBD is

*To whom correspondence should be addressed.
Tel: +86-22-2350-7022, Fax: +86-22-2350-7022,
E-mail: xzfeng@nankai.edu.cn

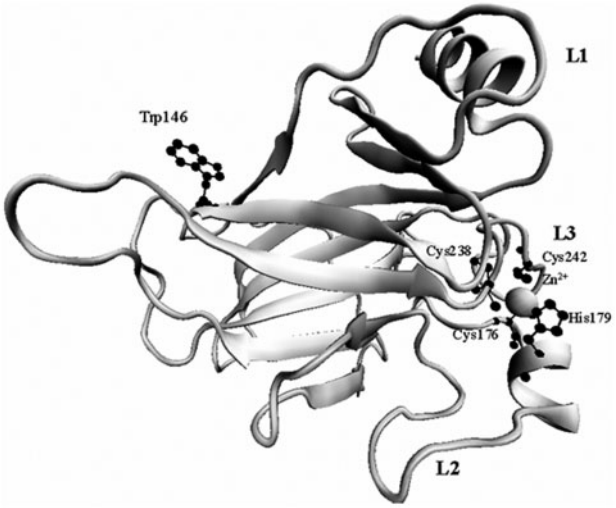

Fig. 1. **X-ray crystal structure of p53DBD (*20*).** Residues coordinated zinc ion are labeled and shown as stick models. Trp-146 is also shown, which was used as a fluorescent probe for denaturation assays.

enhanced after binding the two metal ions by using denaturation assays and fluorescence spectroscopy. The data represent here and, together with previous studies (*23–26*, *29*), demonstrate that metal ions play a dual modulatory role in p53DBD. The metal ions not only support the DNA-binding affinity of p53DBD, but also stabilize the structure of the protein.

MATERIALS AND METHODS

Expression and Purification of p53DBD—The p53DBD cDNA encoding amino acid residues 96–308 was cloned in the pET32a expression vector (Novagen). The recombinant plasmids were transformed into *Escherichia coli* BL21 (DE3) trx B^-. The cells were incubated in LB medium at 37°C and induced by 0.25 mM isopropyl β-D-thiogalactoside (IPTG) and then cultured at 25°C for 7 h. The cells were harvested by centrifugation and lysed by osmotic shock method. The recombinant proteins were purified by two chromatographic steps: affinity chromatography and gel filtration chromatography. The pooled fractions from the gel filtration column were digested with enterokinase at 25°C for 7 h. The digested protein was further purified further on a Sephadex G-75 gel filtration column in buffer G (50 mM Tris–HCl, pH 7.5, 100 mM NaCl, 1 mM DTT). The final purified p53DBD was checked on an SDS–polyacrylamide gel for purity. The protein concentration was determined by the Bradford method with bovine serum albumin as the standard. Apo-DBD was prepared by treating p53DBD with 2.5 mM EDTA, and then passed through a column of Sephadex G-75, which equilibrated in buffer G.

Equilibrium Unfolding Experiments—Denaturation assays were performed on a Hitachi F-4500 fluorescence spectrophotometer using an excitation wavelength of 295 nm at 10°C. Emission spectra were recorded from 310 to 450 nm. The excitation and the emission bandwidths were both set at 5 nm. Each data point reported was an average of three determinations. The protein concentration was adjusted to 1.8 μM in buffer G (50 mM Tris–HCl, pH 7.5, 100 mM NaCl, 1 mM DTT) (apo-DBD) containing 100 μM $MgCl_2$ (Mg^{2+}-DBD), or 100 μM $ZnCl_2$ (Zn^{2+}-DBD).The protein solutions were then denatured with various concentrations of GdmHCl for 5 h at 10°C. All spectra were corrected by subtracting the signals from buffer containing the appropriate quantity of substrate.

The parameter ΔGu can be described in Equation (1),

$$\Delta G_u = -RT \ln K_u \quad (1)$$

where ΔGu is the apparent free energy of unfolding in the presence of denaturant, R is the gas constant and T is the absolute temperature in kelvins. For a two-state unfolding process, from moderate to high denaturant concentrations the apparent free energy of unfolding (ΔG_u^0) is linearly dependent on the molar concentration of the denaturant according to Equation (2),

$$\Delta G_u = \Delta G_u^0 - m[GdmHCl] \quad (2)$$

where ΔG_u^0 is the free energy of unfolding in the absence of denaturant and m is the cooperativity of unfolding. ΔG_u^0 and m will be derived from the intercept and slope of a linear plot of ΔG_u versus [GdmHCl] based on Equation (2).

Differential Scanning Calorimetry (DSC) Measurement—DSC measurements were carried out on a NETZSCH DSC-204 differential scanning calorimeter (NETZSCH). Temperatures from 4 to 55°C were scanned at a rate of 1°C/min. The p53DBD (35 μM) in buffer G (50 mM Tris–HCl, pH 7.5, 100 mM NaCl, 1 mM DTT) (apo-DBD) incubated with 100 μM Mg^{2+} (Mg^{2+}-DBD) and Zn^{2+} (Zn^{2+}-DBD) for 30 min on ice. The buffer was used for baseline scans and the system was allowed to equilibrate at 4°C for 20 min before scanning. The apparent T_m values of p53DBD with and without metal ions were determined.

1-Anilino-8-Naphthalenesulphonate (ANS)-Binding Measurements—Binding of 1-anilino-8-naphthalenesulphonate (ANS) to the protein was accessed by measuring the fluorescence enhancement of ANS. The excitation wavelength was set at 380 nm, and the emission spectra were scanned from 400 to 600 nm. All measurements were corrected by subtracting the fluorescence intensity of the buffer.

Quenching of p53DBD by Acrylamide—Quenching experiments were performed at 10°C by continuously adding aliquots of the concentrated acrylamide stock solution (10 M, pH 7.5) to the protein solution. The excitation wavelength was set at 295 nm and the fluorescence emission spectra were scanned from 310 to 400 nm. The integration area between 330 and 360 nm was used for data analysis. The fluorescence quenching data in the presence of acrylamide was analysed according to the Stern–Volmer equation shown in Equation (3) (*30–32*),

$$\frac{F_0}{F} = 1 + K_{sv} \cdot [Q] \quad (3)$$

where F_0 and F are the fluorescence intensities in the absence and presence of the quencher, respectively. K_{sv} is

the dynamic Stern–Volmer quenching constant, and [*Q*] is the quencher concentration.

When the Stern–Volmer plot displayed an upward curvature, the static quenching concept was used and the experimental data were fitted to a revised Stern–Volmer equation shown in Equation (4) (*30–33*),

$$\frac{F_0}{F} = (1 + K_{sv} \cdot [Q]) \exp(V[Q]) \quad (4)$$

where V is the static quenching constant measuring the complex formation between acrylamide and the protein.

RESULTS

Expression, Purification and Intrinsic Fluorescence Properties of the p53DBD Protein—To evaluate the role of metal ions on the structural stability of p53DBD, a truncated form of p53DBD encoding amino acid residues 96–308 was expressed and purified (*34–36*). SDS–PAGE analysis showed that the 24-kDa p53DBD protein was the predominant polypeptide in the purified fractions (Fig. 2A). The intrinsic fluorescence of the tryptophan residue can be used as a sensitive probe to monitor the conformational change of p53DBD. The fluorescence properties of the purified apo-DBD in buffer G at room temperature were shown in Fig. 2B. Analysis of the background-corrected fluorescence emission spectra of apo-DBD showed that the recombinant protein exhibited a fluorescence spectrum with a maximum at 340 nm when excited at 295 nm. After denaturing with 4.2 M GdmHCl for 5 h, there was a distinct red shifting of the maximum emission fluorescence to 352 nm and the fluorescence intensity decreased at the same time. The fluorescence signals thus provide direct method in monitoring the conformational changes of p53DBD during the unfolding process.

GdmHCl-Induced Equilibrium Unfolding of p53DBD—The effect of metal ions on the p53DBD structural stability was evaluated by GdmHCl-induced equilibrium unfolding assays performed at 10°C. The maximum fluorescence emission wavelength of the apo-DBD shifted from 340 to 352 nm upon an increase of the GdmHCl concentration (Fig. 2B), reflecting tryptophan residues transferred to a more polar environment. The structure of the apo-DBD was very sensitive to the small concentration changes of GdmHCl in the lower concentration range between 1.0 and 3.0 M and the strongest effects on emission changes were observed in this range (Fig. 3A). No changes could be observed at GdmHCl concentrations higher than 3.0 M. The C_m value (midpoint concentration of denaturant required to unfold half of the protein) was 1.79 M. The Mg^{2+}-DBD and Zn^{2+}-DBD were also analysed by similar equilibrium unfolding assays. The equilibrium unfolding data in Fig. 3A were fitted to the two-state model. The plots of ΔG_u versus *[GdmHCl]* are shown in Fig. 3B. The complete thermodynamic unfolding parameters were determined, and the values were presented in Table 1. The present data (Table 1) showed a dependence of C_m and $\Delta G_u{}^0$ on the presence of the metal ions. Midpoint concentrations (C_m) of GdmHCl were found to increase from apoDBD to ion-bound forms. The free energy of unfolding ($\Delta G_u{}^0$) of Mg^{2+}-DBD and Zn^{2+}-DBD increased by 1.74 and 4.60 kJ mol^{-1}, respectively. These results suggested that the binding of metal ions increased the stability of p53DBD.

Effects of Metal Ions on Apparent T_m of p53DBD—The effects of metal binding on the thermal stability of p53DBD were also assessed by DSC scans (Fig. 4). Thermal denaturation of apo-DBD revealed a midpoint of thermal transition (T_m) of 39.6°C. The addition of Zn^{2+} resulted in a shift of the T_m value to 43.1°C. Similarly, the addition of Mg^{2+} was found to raise the T_m value to 40.7°C. These results demonstrated that

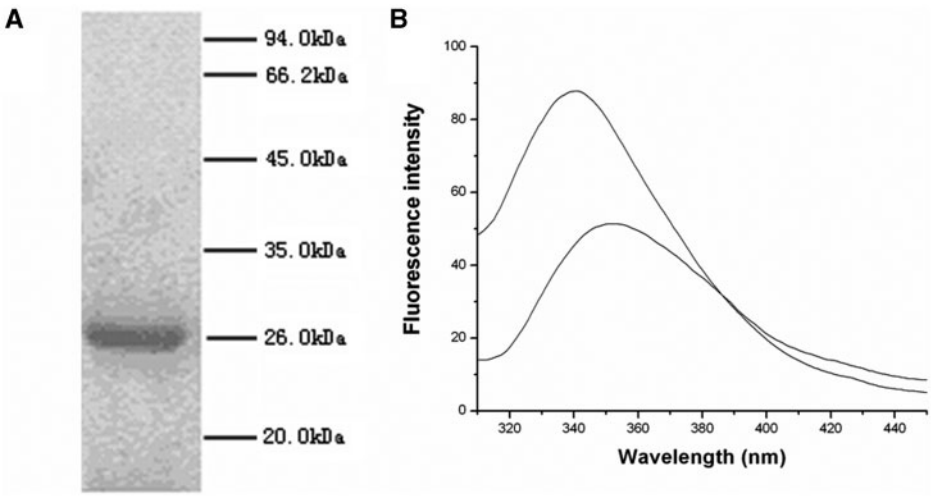

Fig. 2. **Expression, purification and intrinsic fluorescence properties of p53DBD.** (A) The purified p53DBD was analysed by electrophoresis through a 12.5% polyacrylamide gel containing 0.1% SDS and visualized with Coomassie blue dye. The positions and sizes (in kilodalton) of the size markers are indicated on the right. (B) Background-corrected fluorescence emission spectrum of the apo-DBD. The upper curve: 1.8 μM apo-DBD in 50 mM Tris–HCl, pH 7.5, 100 mM NaCl, 1 mM dithiothreitol at room temperature. The lower curve: 1.8 μM apo-DBD was treated with 4.2-M GdmHCl for 1 h at room temperature. Fluorescence spectrum was recorded at an excitation wavelength of 295 nm.

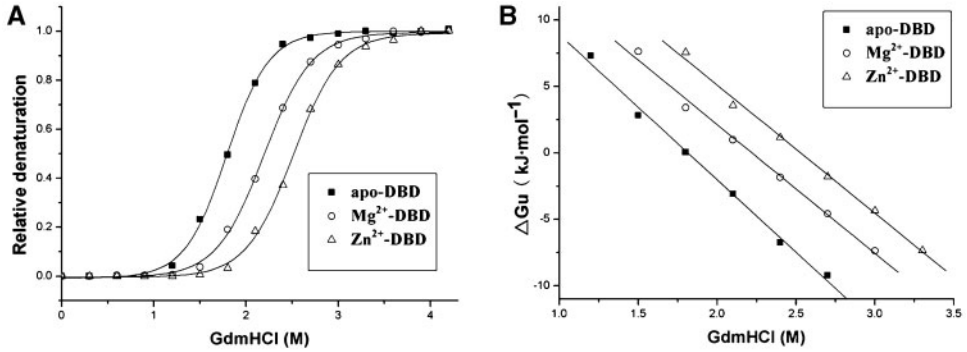

Fig. 3. **GdmHCl-induced unfolding equilibrium of the p53DBD protein.** (A) Transition curves for GdmHCl-induced unfolding of apo-DBD (filled square), Mg^{2+}-DBD (open circle) and Zn^{2+}-DBD (open triangle). (B) The linear plot of ΔG_u versus [*GdmHCl*] based on Equation (2).

Table 1. **Thermodynamic unfolding parameters determined by equilibrium GdmHCl denaturation.**

Protein	C_m M	ΔC_m M	m kJ mol^{-1} M^{-1}	ΔG_u^0 kJ mol^{-1}	$\Delta\Delta G_u^0$ kJ mol^{-1}
apo-DBD	1.79	0.00	10.90	19.77	0.00
Mg^{2+}-DBD	2.19	0.40	9.69	21.51	1.74
Zn^{2+}-DBD	2.51	0.72	9.63	24.37	4.60

The parameters ΔG_u^0 (Gibbs free energy of unfolding in the absence of denaturant), m (cooperativity of unfolding) and C_m (midpoint concentration of denaturant required to unfold half of the protein) were determined by *GdmHCl* denaturation. The differences in C_m and $\Delta\Delta G_u^0$ values compared with the free p53DBD protein are also shown (ΔC_m and $\Delta\Delta G_u^0$, respectively).

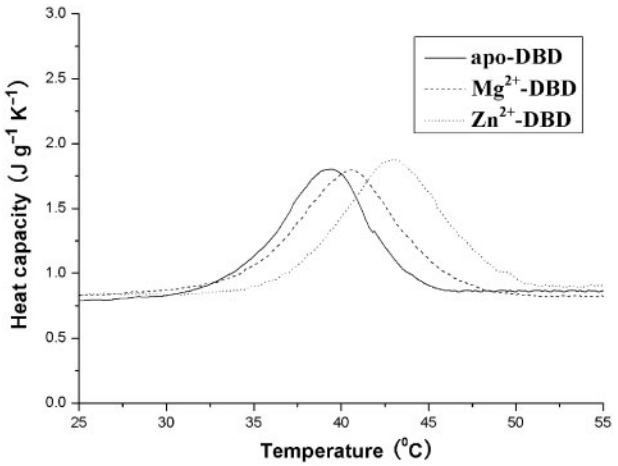

Fig. 4. **Apparent melting temperatures of p53DBD in the absence and presence of metal ions.**

the binding of metal ions to p53DBD increased the thermal stability of the protein.

Binding of Metal Ions Increases Hydrophobic Exposure of p53DBD—To obtain additional information of structural changes after the binding of metal ions, we investigated the binding of structural fluorescent probes to the p53DBD protein. The exposure of the hydrophobic area of the p53DBD protein was accessed by measuring the ANS binding. The aromatic chromophore ANS is weakly fluorescent in aqueous buffer but exhibits a marked increase in emission upon binding to hydrophobic domains in proteins. Thus, ANS can be used as a probe to measure exposed hydrophobic surfaces on proteins (*37*, *38*). Analysis of the fluorescent spectra in Fig. 5A revealed that the apo-DBD bound to ANS very weakly, which suggested that there were limited hydrophobic regions at the surface of the protein. Nevertheless, when p53DBD was incubated with 100 μM Mg^{2+}/Zn^{2+}, there was a significant enhancement of ANS fluorescence. This implied that the hydrophobic exposure of p53DBD was increased upon metal ions binding.

It is interesting to further explore the hydrophobic exposure of the p53DBD protein during urea denaturation. As can be seen in Fig. 5B, when the apo-DBD incubated with increasing concentrations of urea, the fluorescence emission intensity of ANS had little change. However, there was a distinct decrease of the emission intensity when ion-bound forms treated with increasing concentrations of urea. It was due to that Mg^{2+}- or Zn^{2+}-bound form became unfolded under the effect of the denaturant. Overall, all of these results indicated that the binding of metal ions enhanced hydrophobic exposure on the p53DBD surface.

Conformational Changes of p53DBD upon the Binding of Metal Ions during Urea Denaturation—To further characterize the conformational changes upon the binding of metal ions, the intrinsic fluorescence of the protein was examined by quenching it with acrylamide. Acrylamide is an efficient quencher of tryptophan fluorescence in proteins, which can penetrate into the interior of the protein matrix (*39*). According to Equation (4), the increasing rate of F_0/F could represent the accessibility to acrylamide. In the absence of urea, F_0/F of apo-DBD was increasing much faster than Mg^{2+}-DBD or Zn^{2+}-DBD (Fig. 6A), which means that the apo-DBD displayed greater accessibility for acrylamide than Mg^{2+}-DBD or Zn^{2+}-DBD. In other words, acrylamide exhibited a decreased access to the interior of ions-bound forms. It suggested that the binding of metal ions to the p53DBD induced a structure modification of the protein and provided significant protection against acrylamide quenching. The various quenching constants are summarized in Table 2.

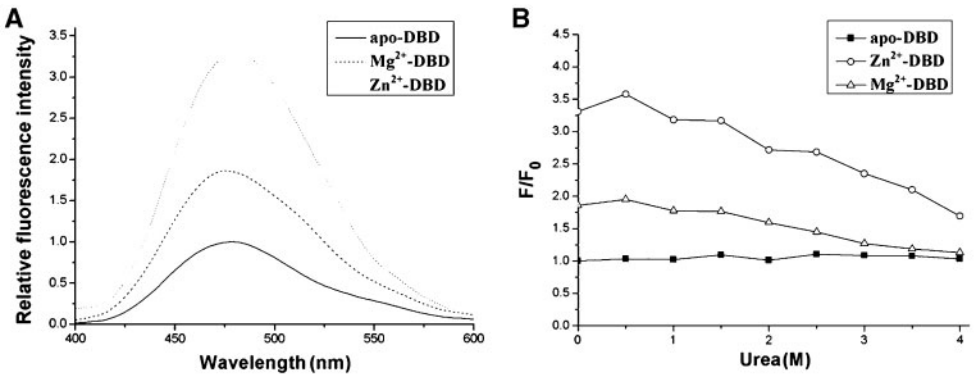

Fig. 5. **Binding of ANS to p53DBD during urea denaturation.** (A) ANS fluorescence spectra of apo-DBD, Mg^{2+}-DBD and Zn^{2+}-DBD, as indicated on the curves. (B) The apo-DBD (filled square), Mg^{2+}-DBD (open triangle) and Zn^{2+}-DBD (open circle) were incubated with various concentrations of urea at 10°C for 5 h. Fluorescence emission was monitored after the addition of 50 μM ANS at an excitation wavelength of 380 nm. The integrated fluorescence area between 420 and 560 nm was evaluated.

The acrylamide quenching experiments were then performed in the presence of increasing urea concentrations. Because of the effect of increasing amount of denaturant, tryptophan in unfolded p53DBD was more exposed to the solvent molecules and to quencher; F_0/F was increasing much faster (Fig. 6) and the values of V and K_{SV} became bigger (Table 2) when the concentration quencher increased. When the concentration of urea more than 6 M, the upward curvature and the values of K_{SV} were no more changed (data not shown), which suggested that the value of 8.0–8.7 (K_{sv}) means the fully accessibility to Trp. At lower concentration of urea (Fig. 6A–C), the binding of metal ions provided significant protection against acrylamide quenching. This protection was reduced at higher concentration of urea (Fig. 6D and E). The acrylamide quenching assays indicated that the binding of metal ions to the p53DBD increased the structural stability of the protein.

DISCUSSION

Metal ions are needed by at least one-quarter of all proteins (*40–42*). Metal ions perform a variety of tasks in cells from structural stabilization to enzyme catalysis (*43*, *44*). The tumour suppressor protein p53 is a zinc-bound transcription factor (*20–22*). Nevertheless, the binding of other metal ions can affect the structure and DNA-binding activity of p53 (*27–28*). In our recent study, we found that magnesium ions could bind to the p53DBD protein and enhanced the DNA-binding affinity of p53DBD in a non-specific manner (*29*).

In this study, a systematic analysis of the conformation and stability changes induced by these two metal ions was reported. The denaturation assays clearly demonstrated that the protein exhibited an increased structural stability in the presence of metal ions, compared with the apo-DBD (Fig. 3). The stability against chemical denaturation increased in the order apo < Mg^{2+} < Zn^{2+}. The DSC scans showed that the binding of metal ions also increased the thermal stability of p53DBD (Fig. 4). The enhancement of Mg^{2+} on the structural stability of p53DBD is weaker than that of Zn^{2+}. 'Soft' ions, such as Cd^{2+} and Hg^{2+}, have a high polarizability and they form stable bonds with polarizable ligands such as sulfur. In contrast, 'Hard' ions, such as Mg^{2+} and Ca^{2+}, possess a low polarizability but a high positive charge, and they interact with ligands through electrostatic forces. Zn^{2+} possesses intermediate properties between 'hard' and 'soft' (*45*). Zinc-binding site is composed of three Cys and one His residues in p53DBD. It is apprehensible that zinc is easier to bind the protein than magnesium. Actually, the binding affinity of Zn^{2+} to p53DBD is 9-fold greater than that of Mg^{2+} (*29*)]. It is understandable that Mg^{2+} confers a weaker stability contribution than Zn^{2+}.

Previous studies have shown that a conformational change induced by metal ions is required to support the DNA-binding activity (*23–26*). The NMR spectra showed that residues near the Zn^{2+}-binding site exhibited widespread shifts and the minor-groove-binding loop formed upon the binding of metal ions (*26*). Binding of the metal ion induced rearrangement at the DNA-binding surface and thus changed DNA-binding affinity (*26*). Our study clearly showed that the binding of metal ions induced a conformational change that was characterized by an increased exposure of hydrophobic regions (Fig. 5). This conformational modification may lead to DNA-binding surface rearrangements, which influence the DNA-binding activity of p53DBD. The coordination polyhedron of catalytic zinc is usually dominated by histidine side chains, while the coordination polyhedron of structural zinc is almost exclusively dominated by cysteine thiolates (*45*). In p53DBD, Zn^{2+} is coordinated by cysteines 176, 238 and 242 and His179 (*20*). Zinc coordination keeps the L2 and the DNA binding L3 loops together and holds the L3 loop in the proper orientation for the DNA minor groove binding. At the same time, zinc coordination enhances the structural stability of p53DBD (*26*). For Mg^{2+}, competitive binding assays displayed that Mg^{2+} bind to the same active site of Zn^{2+} on the protein (*29*). Mg^{2+}-mediated binding of p53DBD to the DNA sites is through allosteric activation that the binding of Mg^{2+} induces conformational changes in p53DBD. On the other hand, Mg^{2+} binds to DNA that makes it a suitable substrate and enhances the DNA-binding affinity of p53DBD in a sequence-independent manner (*29*).

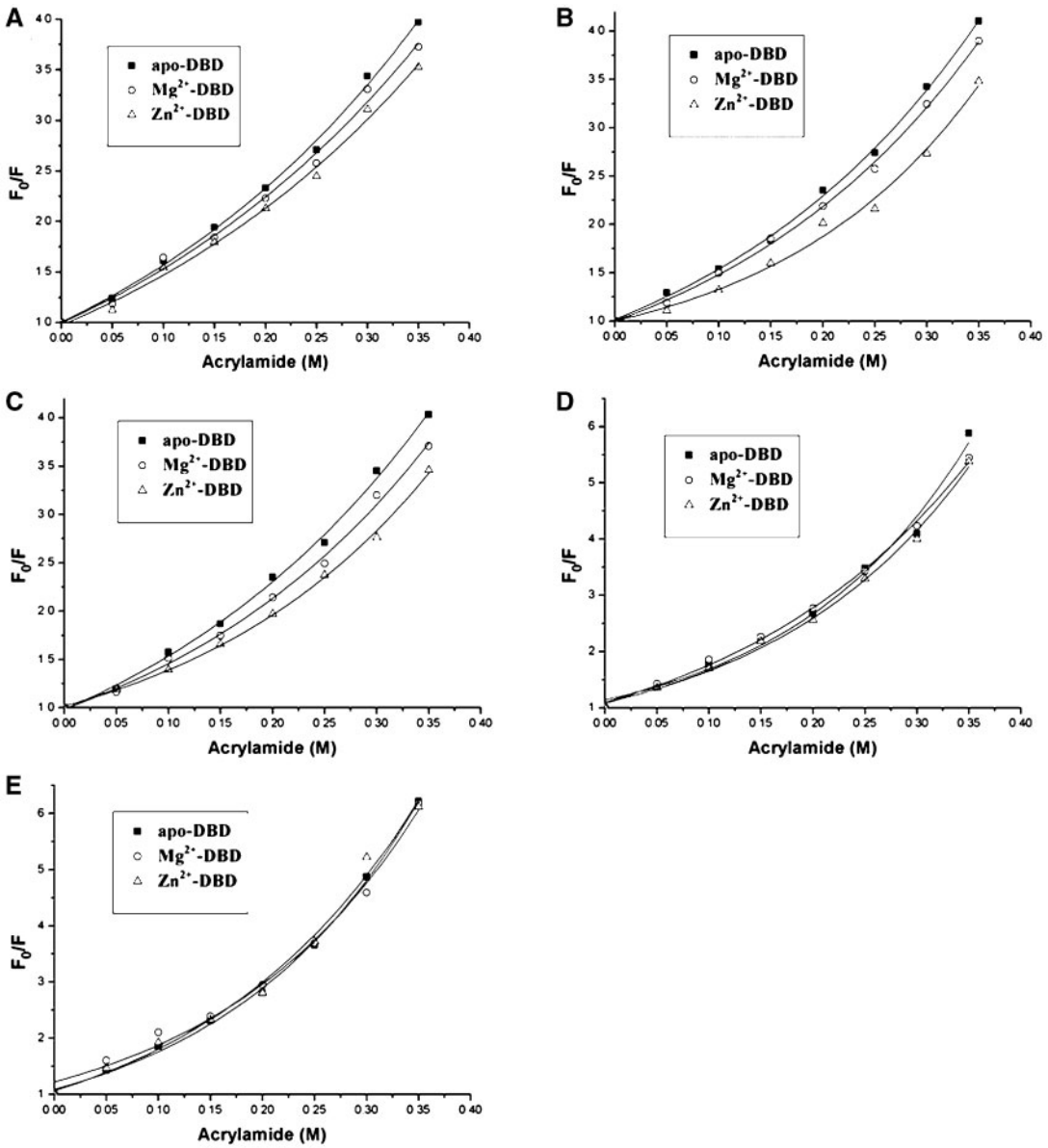

Fig. 6. **Stern–Volmer plots for the quenching of the intrinsic fluorescence of the p53DBD protein by acrylamide.** The apo-DBD (filled square), Mg^{2+}-DBD (open circle) and Zn^{2+}-DBD (open triangle) were denatured with 0 M (A), 1 M (B), 2 M (C), 4 M (D) and 6 M (E) urea at 10°C for 5 h. The denatured protein was then titrated with various amounts of acrylamide. Excitation was set at 295 nm, and the emission of the fluorescence-integrated area between 330 and 360 nm was calculated.

Table 2. **Quenching of the intrinsic fluorescence of apo-DBD, Mg^{2+}-DBD and Zn^{2+}-DBD by acrylamide.**

Urea concentration	V			K_{SV}		
	apo-DBD	Mg^{2+}-DBD	Zn^{2+}-DBD	apo-DBD	Mg^{2+}-DBD	Zn^{2+}-DBD
	M		M^{-1}	$s^{-1}M^{-1}$		
0	1.119	1.068	1.023	4.818	4.536	4.297
1	1.258	1.216	1.062	4.833	4.377	4.182
2	1.267	1.233	1.085	4.958	4.463	4.226
4	1.322	0.892	1.262	6.961	7.214	6.535
6	1.287	1.063	1.145	8.073	8.342	8.746

Fluorescence spectroscopy assays were performed to evaluate the dynamic Stern–Volmer quenching constant (K_{SV}) and the static quenching constant (V).

In this work, we discovered that the binding of Mg^{2+} could enhance the structural stability of p53DBD. Over all, these results suggests that the metal ion-induced conformational change is necessary to support for its DNA-binding activity by rearranging the side chains of residues located in the active site of protein, while at the same time contributing to the stabilization of the protein architecture. Therefore, we propose that metal ions play a dual modulatory role in the process of p53DBD functioning as a transcription factor.

CONCLUSION

The novel aspect of the current study is that we demonstrate the structural roles of metal ions in the p53DBD protein. The p53DBD protein undergoes a conformational change upon the binding of metal ions, which is characterized by an increased stability of the protein. The data represent here and, together with previous studies (*23–26*, *29*), demonstrate that metal ions play a dual modulatory role in p53DBD. The metal ions not only support the DNA-binding affinity of p53DBD, but also stabilize the structure of the protein.

FUNDING

National Natural Science Foundation of China (Grant No. 90403140).

CONFLICT OF INTEREST

None declared.

REFERENCES

1. Lane, D.P. (1992) p53, guardian of the genome. *Nature* **358**, 15–16
2. Levine, A.J. (1993) The tumor suppressor genes. *Annu. Rev. Biochem.* **62**, 623–651
3. Ko, L.J. and Prives, C. (1996) p53: puzzle and paradigm. *Genes Dev.* **10**, 1054–1072
4. Levine, A.J. (1997) p53, the cellular gatekeeper for growth and division. *Cell* **88**, 323–331
5. Ding, H.F. and Fisher, D.E. (1998) Mechanisms of p53-mediated apoptosis. *Crit. Rev. Oncog.* **9**, 83–98
6. Barak, Y., Juven, T., Haffner, R., and Oren, M. (1993) mdm2 expression is induced by wild type p53 activity. *EMBO J.* **12**, 461–468
7. Kastan, M.B., Zhan, Q., El-Deiry, W.S., Carrier, F., Jacks, T., Walsh, W.V., Plunkett, B.S., Vogelstein, B., and Fornace, A.J. (1992) A mammalian cell cycle checkpoint pathway utilizing p53 and GADD45 is defective in ataxia-telangiectasia. *Cell* **71**, 587–597
8. El-Deiry, W.S., Tokino, T., Velculescu, V.E., Levy, D.B., Parsons, R., Trent, J.M., Lin, D., Mercer, W.E., Kinzler, K.W., and Vogelstein, B. (1993) WAF1, a potential mediator of p53 tumor suppression. *Cell* **75**, 817–825
9. Harper, J.W., Adami, G.R., Wei, N., Keyomarsi, K., and Elledge, S.J. (1993) The p21 Cdk-interacting protein Cip1 is a potent inhibitor of G1 cyclin-dependent kinases. *Cell* **75**, 805–816
10. Miyashita, T. and Reed, J.C. (1995) Tumor suppressor p53 is a direct transcriptional activator of the human bax gene. *Cell* **80**, 293–299
11. Horikoshi, N., Usheva, A., Chen, J.D., Levine, A.J., Weinmann, R., and Shenk, T. (1995) Two domains of p53 interact with the TATA-binding protein, and the adenovirus 13S E1A protein disrupts the association, relieving p53-mediated transcriptional repression. *Mol. Cell Biol.* **15**, 227–234
12. Bargonetti, J., Friedman, P.N., Kern, S.E., Vogelstein, B., and Prives, C. (1991) Wild-type but not mutant p53 immunopurified proteins bind to sequences adjacent to the SV40 origin of replication. *Cell* **65**, 1083–1091
13. Dutta, A., Ruppert, J.M., Aster, J.C., and Winchester, E. (1993) Inhibition of DNA replication factor RPA by p53. *Nature* **365**, 79–82
14. Prives, C. (1994) How loops, β sheets, and α helices help us to understand p53. *Cell* **78**, 543–546
15. Milner, J. (1994) Forms and functions of p53. *Semin. Cancer Biol.* **5**, 211–219
16. Anderson, M.E. and Tegtmeyer, P. (1995) Giant leap for p53, small step for drug design. *BioEssays* **17**, 3–7
17. Bargonetti, J., Manfredi, J.J., Chen, X., Marshak, D.R., and Prives, C. (1993) A proteolytic fragment from the central region of p53 has marked sequence-specific DNA-binding activity when generated from wild-type but not from oncogenic mutant p53 protein. *Genes Dev.* **7**, 2565–2574
18. Pietenpol, J.A., Tokino, T., Thiagalingam, S., El-Diery, W.S., Kinzler, K.W., and Vogelstein, B. (1994) Sequence-specific transcriptional activation is essential for growth suppression by p53. *Proc. Natl Acad. Sci. USA* **91**, 1998–2002
19. Meek, D.W. (1998) Multisite phosphorylation and the integration of stass signals at p53. *Cell. Signal.* **10**, 159–166
20. Cho, Y., Gorina, S., Jeffrey, P.D., and Pavletich, N.P. (1994) Crystal structure of a p53 tumor suppressor-DNA complex: understanding tumorigenic mutations. *Science* **265**, 346–355
21. Pavletich, N.P., Chambers, K.A., and Pabo, C.O. (1993) The DNA-binding domain of p53 contains the four conserved regions and the major mutation hot spots. *Genes Dev.* **7**, 2556–2564
22. Ho, W.C., Fitzgerald, M.X., and Marmorstein, R. (2006) Structure of the p53 core domain dimer bound to DNA. *J. Biol. Chem.* **281**, 20494–20502
23. Hainaut, P. and Milner, J. (1993) A structural role for metal ions in the "wild-type" conformation of the tumor suppressor protein p53. *Cancer Res.* **53**, 1739–1742
24. Verhaegh, G.W., Parat, M.O., Richard, M.J., and Hainaut, P. (1998) Modulation of p53 protein conformation and DNA-binding activity by intracellular chelation of zinc. *Mol. Carcinog.* **21**, 205–214
25. Meplan, C., Richard, M.J., and Hainaut, P. (2000) Metalloregulation of the tumor suppressor protein p53: zinc mediates the renaturation of p53 after exposure to metal chelators in vitro and in intact cells. *Oncogene* **19**, 5227–5236
26. Butler, J.S. and Loh, S.N. (2003) Structure, function, and aggregation of the zinc-free form of the p53 DNA binding domain. *Biochemistry* **42**, 2396–2403
27. Hainaut, P., Rolley, N., Davies, M., and Milner, J. (1995) Modulation by copper of p53 conformation and sequence-specific DNA binding: role for Cu(II)/Cu(I) redox mechanism. *Oncogene* **10**, 27–32
28. Verhaegh, G.W., Richard, M.J., and Hainaut, P. (1997) Regulation of p53 by metal ions and by antioxidants: dithiocarbamate down-regulates p53 DNA-binding activity by increasing the intracellular level of copper. *Mol. Cell. Biol.* **17**, 5699–5706
29. Xue, Y.L., Wang, S., and Feng, X.Z. (in press) Influence of magnesium ion on the binding of p53 DNA binding domain to DNA response elements. *J. Biochem.*
30. Eftink, M.R. and Ghiron, C.A. (1976) Exposure of tryptophanyl residues in proteins. quantitative determination by fluorescence quenching studies. *Biochemistry* **15**, 672–680
31. Eftink, M.R. and Ghiron, C.A. (1981) Fluorescence quenching studies with proteins. *Anal. Biochem.* **114**, 199–227

32. Chang, H.C., Chou, W.Y., and Chang, G.G. (2002) Effect of metal binding on the structural stability of pigeon liver malic enzyme. *J. Biol. Chem.* **277**, 4663–4671
33. Benzaghou, I., Bougie, I., and Bisaillon, M. (2004) Effect of metal ion binding on the structural stability of the hepatitis C virus RNA polymerase. *J. Biol. Chem.* **279**, 49755–49761
34. Balagurumoorthy, P., Sakamoto, H., Lewis, M.S., Zambrano, N., Clore, G.M., Gronenborn, A.M., Appella, E., and Harrington, R.E. (1995) Four p53 DNA-binding domain peptides bind natural p53-response elements and bend the DNA. *Proc. Natl Acad. Sci. USA* **92**, 8591–8595
35. Nagaich, A.K., Appella, E., and Harrington, R.E. (1997) DNA bending is essential for the site-specific recognition of DNA response elements by the DNA binding domain of the tumor suppressor protein p53. *J. Biol. Chem.* **272**, 14842–14849
36. Nagaich, A.K., Zhurkin, V.B., Durell, S.R., Jernigan, R.L., Appella, E., and Harrington, R.E. (1997) p53-induced DNA bending and twisting: p53 tetramer binds on the outer side of a DNA loop and increases DNA twisting. *Proc. Natl Acad. Sci. USA* **96**, 1875–1880
37. Slavik, J. (1982) Anilinonaphtalene sulfonate as a probe of membrane composition and function. *Biochim. Biophys. Acta* **694**, 1–25
38. Labowicz, J.R. (1999) *Principles of Fluorescence Spectroscopy*, pp. 237–266, Kluwer/Plenum, New York
39. Calhoun, D.B., Vanderkooi, J.M., and Englander, S.W. (1983) Penetration of small molecules into proteins studied by quenching of phosphorescence and fluorescence. *Biochemistry* **22**, 1533–1539
40. Rosenzweig, A.C. (2002) Metallochaperones: bind and deliver. *Chem. Biol.* **9**, 673–677
41. Ferrer, M., Golyshina, O.V., Beloqui, A., Golyshin, P.N., and Timmis, K.N. (2007) The cellular machinery of Ferroplasma acidiphilum is iron-protein-dominated. *Nature* **445**, 91–94
42. Tottey, S., Waldron, K.J., Firbank, S.J., Reale, B., Bessant, C., Sato, K., Cheek, T.R., Gray, J., Banfield, M.J., Dennison, C., and Robinson, N.J. (2008) Protein-folding location can regulat manganese binding versus copper- or zinc-binding. *Nature* **455**, 1138–1142
43. Berg, J.M. and Godwin, H.A. (1997) Lessons from zinc-binding peptides. *Annu. Rev. Biophys. Biomol. Struct.* **26**, 357–371
44. Thomson, A.J. and Gray, H.B. (1998) Bio-inorganic chemistry. *Curr. Opin. Chem. Biol.* **2**, 155–158
45. Christianson, D.W. (1991) Structural biology of zinc. *Adv. Protein Chem.* **42**, 281–355